Angiogenesis (2011) 14:255–266
DOI 10.1007/s10456-011-9210-8

ORIGINAL PAPER

# Effect of MDM2 and vascular endothelial growth factor inhibition on tumor angiogenesis and metastasis in neuroblastoma

**Danielle M. Patterson · Dongbing Gao · Denae N. Trahan · Brett A. Johnson · Andrew Ludwig · Eveline Barbieri · Zaowen Chen · Jose Diaz-Miron · Lyubomir Vassilev · Jason M. Shohet · Eugene S. Kim**

Received: 24 February 2011 / Accepted: 28 March 2011 / Published online: 12 April 2011


**Abstract** Neuroblastoma is the most common pediatric abdominal tumor and principally a p53 wild-type, highly vascular, aggressive tumor, with limited response to anti-VEGF therapies alone. MDM2 is a key inhibitor of p53 and a positive activator of hypoxia-inducible factor-1α (HIF-1α) and vascular endothelial growth factor (VEGF) activity with an important role in neuroblastoma pathogenesis. We hypothesized that concurrent inhibition of both MDM2 and VEGF signaling would have cooperative anti-tumor effects, potentiating anti-angiogenic strategies for neuroblastoma and other p53 wild-type tumors. We orthotopically implanted SH-SY5Y neuroblastoma cells into nude mice ($n = 40$) and treated as follows: control, bevacizumab, Nutlin-3a, combination of bevacizumab plus Nutlin-3a. Expression of HIF-1α and VEGF were measured by qPCR, Western blot, and ELISA. Tumor apoptosis was measured by immunohistochemistry and caspase assay. Angiogenesis was evaluated by immunohistochemistry for vascular markers (CD-31, type-IV collagen, αSMA). Both angiogenesis and metastatic burden were digitally quantified. In vitro, Nutlin-3a suppresses HIF-1α expression with subsequent downregulation of VEGF. Bevacizumab plus Nutlin-3a leads to significant suppression of tumor growth compared to control ($P < 0.01$) or either agent alone. Combination treated xenograft tumors display a marked decrease in endothelial cells ($P < 0.0001$), perivascular basement membrane ($P < 0.04$), and vascular mural cells ($P < 0.004$). Nutlin-3a alone and in combination with bevacizumab leads to significant tumor apoptosis ($P < 0.0001$ for both) and significant decrease in incidence of metastasis ($P < 0.05$) and metastatic burden ($P < 0.03$). Bevacizumab plus Nutlin-3a cooperatively inhibits tumor growth and angiogenesis in neuroblastoma in vivo with dramatic effects on tumor vascularity. Concomitantly targeting VEGF and p53 pathways potently suppresses tumor growth, and these results support further clinical development of this approach.

**Keywords** Neuroblastoma · Nutlin · Bevacizumab · Angiogenesis · Metastasis

J. M. Shohet and E. S. Kim are co-senior authors—both senior authors contributed equally to this work.

**Electronic supplementary material** The online version of this article (doi:10.1007/s10456-011-9210-8) contains supplementary material, which is available to authorized users.

D. M. Patterson · B. A. Johnson · J. Diaz-Miron · E. S. Kim (✉)
Michael E. Debakey Department of Surgery, Division of Pediatric Surgery, Baylor College of Medicine, Texas Children's Hospital, CCC Building, Suite 650, 6701 Fannin, Houston, TX 77030, USA
e-mail: eskim@bcm.edu

D. Gao · D. N. Trahan · A. Ludwig · E. Barbieri · Z. Chen · J. M. Shohet · E. S. Kim
Department of Pediatrics, Texas Children's Cancer Center, and Center for Cell and Gene Therapy, Baylor College of Medicine, Houston, TX 77030, USA

L. Vassilev
Department of Discovery Oncology, Roche Research Center, Hoffmann–La Roche, Inc., Nutley, NJ 07110, USA

## Introduction

Neuroblastoma is the most common pediatric extracranial solid tumor and accounts for almost 15% of all pediatric cancer mortalities. Despite aggressive chemotherapy and radiation protocols, survival remains poor for children with high-risk disease [1, 2]. Current chemotherapy regimens

are highly toxic with severe morbidity and risk of secondary malignancy [3–5]. With current treatment protocols, approximately 80% of high-risk patients go into remission [6]. However, long-term survival rates are less than 50% as most of these patients relapse and develop therapy-resistant tumors [7]. This motivates an ongoing effort to develop novel, non-genotoxic targeted therapeutics in order to reduce toxicities and improve survival.

Neuroblastoma is p53 wild-type in >98% of newly diagnosed cases, with functional p53 activity regardless of differentiation status [8, 9]. The primary inhibitor of p53 activity is MDM2, an E3 ubiquitin ligase which is found to be overexpressed in neuroblastoma and other human cancers [10–13]. This is in part due to an activating single nucleotide polymorphism (SNP309) in the MDM2 promoter which confers significant impact on survival in subsets of neuroblastoma and other cancers [14–17]. In addition, we have recently shown that MDM2 plays a role in MYCN-driven neuroblastoma tumorigenesis [18]. Thus, significant interest has developed in the therapeutic application of MDM2 small molecule inhibitors for neuroblastoma and other p53 wild-type cancers [19, 20]. Currently, several small molecule inhibitors that competitively bind MDM2 are under preclinical and clinical investigation [21–23]. Herein, we utilize the small molecule inhibitor Nutlin-3a, which binds to MDM2 and blocks its interaction with p53. This blockade of MDM2 rapidly stabilizes p53 and protects it from ubiquitin-mediated degradation, thus preserving apoptotic pathways [21, 24]. Nutlin has been found to inhibit the growth of both chemosensitive and chemoresistant neuroblastoma cell lines in vivo and in vitro in a p53-dependent manner [19, 24]. In vivo, Nutlin-3 has been shown to significantly suppress tumor growth by p53-mediated tumor apoptosis in subcutaneous tumor models of osteosarcoma and neuroblastoma [19, 21].

MDM2 also has a number of critical p53 independent roles, including functional activation of hypoxia inducible factor-1α (HIF-1α) [25–27]. Hypoxia is a defining characteristic of solid tumors, and HIF-1α plays a central role in tumor adaptation to hypoxia through transcription of a variety of genes such as vascular endothelial growth factor (VEGF) and glycolytic enzymes [28]. Overexpression of MDM2 leads to increased transcriptional activity of HIF-1α [26, 29], while in vitro inhibition of MDM2 by siRNA, antisense oligonucleotides, and Nutlin-3a has demonstrated decreased transcription of downstream targets [27, 30–32]. Most important of these is VEGF, a specific endothelial cell mitogen, permeability and survival factor, which has been found to be overexpressed in almost all human tumors [33].

Antagonism of the VEGF pathway results in inhibition of angiogenesis and tumor growth in a number of tumor model systems [34]. Recently, clinical evidence has validated anti-angiogenic therapies by VEGF blockade as an effective cancer therapy in adult glioblastoma, renal, colorectal, non–small cell lung, and other carcinomas [35–38]. Phase I clinical trials with the VEGF-neutralizing antibody bevacizumab in pediatric patients with refractory solid tumors have demonstrated the safety of treatment in this population [39]. However, many patients with a clinical response to VEGF blockade ultimately develop progressive disease, prompting a search for synergistic agents targeting other elements of tumor angiogenesis [35].

MDM2 inhibition with Nutlin-3a has been demonstrated to have anti-angiogenic activity in in vitro assays [27, 40], but no studies to date have examined the anti-angiogenic effect of Nutlin-3a in an animal cancer model. In this study, we utilize an orthotopic (renal capsule injection) xenograft model of neuroblastoma, which closely recapitulates the highly vascular and invasive growth pattern seen in children, to assess the combined effect of MDM2 inhibition and anti-VEGF antibody therapy on tumor growth and angiogenesis. We demonstrate marked anti-angiogenic activity of Nutlin-3a by suppressing HIF-1α expression and downstream VEGF in neuroblastoma, *independent* of its pro-apoptotic activity mediated through p53. By adding upstream repression of HIF-1α with Nutlin-3a, the efficacy of bevacizumab is increased. Our data support a re-assessment of anti-angiogenic strategies for neuroblastoma and may lead to the development of more effective non-genotoxic approaches to this devastating pediatric malignancy.

## Materials and methods

### Tissue culture and stable lentiviral vectors

The human neuroblastoma cell line SH-SY5Y, previously transfected with a lentivirus, FUW, carrying a luciferase construct (gift of Dr. Darrell Yamashiro, Columbia University, New York) and maintained as described (Supplemental Materials). Xenograft tumors confirmed cells to be neuroblastoma by histology, immunohistochemistry, and flow cytometry for neuroblastoma-specific surface markers, including GD2 and NB-84. RT–PCR was used to confirm expression of the sympathetic neuronal lineage marker, norepinephrine transporter. Cells were grown at 37°C in 5% $CO_2$ until confluent and then harvested by trypsinization, counted with trypan blue staining, and washed and resuspended in sterile saline solution (phosphate buffered saline) at a concentration of $10^7$ per ml.

To generate a p53 knockdown cell line, we used the lentiviral pLSLP vector containing a short-hairpin RNA (shRNA) sequence targeting p53, a kind gift of Dr. Michael

Karin (UCSD, La Jolla, CA). SH-SY5Y cells were infected for 24 h before removal of viral supernatant. Seventy-two hours after transduction cells were grown in media containing 1 μg/ml puromycin to select a stably transduced cell line.

### Antibodies and Western Blot Analysis

Primary antibodies for Western blot analysis are the following: α-HIF-1α (Milipore, Billerica MA), α-CyPB (Santa Cruz Biotechnology). Secondary antibodies used are α-mouse IgG IRDye800, α-rabbit IgG IRDye800, and α-goat IgG IRDye700 (Rockland Immunochemicals, Gilbertsville, PA).

One hundred microgram aliquots of protein from SH-SY5Y cells treated with vehicle (DMSO), Nutlin-3a (5 μM), bevacizumab (1 mg/ml), or combination of Nutlin-3a and bevacizumab were electrophoresed and transferred as described [41]. Human Cyclophilin B was used for loading control in the experiments. The Odyssey Infrared Imaging System (Li-Cor, Lincoln, NE) with the above secondary antibodies were used for detection and desitometry (Odyssey software v3.0, Li-Cor).

### Quantitative real-time PCR

RNA from SH-SY5Y cells was prepared with the RNeasy Plus Mini Kit (Qiagen, Valencia, CA). Quantitative real-time PCR was performed on DNA Engine Opticon Real-Time Cycler (Bio-rad, Hercules, CA) (details in Supplemental Materials).

Primers used are as follows: VEGF-A forward AGG AGGAGGGCAGAATCATCAC, VEGF-A reverse ATGT CCACCAGGGTCTCGATTG, GAPDH forward AAGGT GAAGGTCGGAGTCAA, GAPDH reverse TGGACTCC ACGACGTACTCA.

### Enzyme-linked immunosorbent assay

SH-SY5Y and SH-SH5Y.siP53 cells were plated in 10 cm dishes 24 h prior to the assay. Treated cells were analyzed in triplicate. VEGF-A was measured using the human VEGF Quantikine ELISA Kit (R&D Systems Inc, Minneapolis, MN) according to manufacturer's instructions. Optical density was determined with the DTX 800 multimode detector and analyzed with Multimode Analysis Software (Beckman Coulter, Brea, CA).

### Animal model

The Institutional Animal Care and Use Committee of Baylor College of Medicine approved the experiments described below. An inoculum of $10^6$ SH-SY5Y tumor cells in 0.1 ml of PBS was surgically implanted under the renal capsule of nude mice using a 27-gauge needle (see Supplemental Materials). The MDM2 small molecule inhibitor, Nutlin-3a was administered by oral gavage at a dose of 200 mg/kg twice a day for 14 days. Nutlin-3a vehicle was administered by oral gavage twice a day for 14 days as previously described [21]. Bevacizumab (Genentech, South San Francisco, CA), a humanized anti-VEGF monoclonal antibody, was administered by intraperitoneal injection twice a week for 14 days. All mice tolerated bevacizumab and Nutlin-3a without morbidity.

Xenograft tumors were confirmed to be neuroblastoma by histology, immunohistochemistry, and flow cytometry for neuroblastoma-specific surface markers, including GD2 and NB-84. RT–PCR was used to confirm expression of the sympathetic neuronal lineage marker, norepinephrine transporter.

Starting 1 week after tumor implantation, xenograft tumors from all mice were monitored weekly by bioluminescent imaging (Xenogen IVIS 100 System, Caliper Life Sciences, Hopkinton, MA). The flux (photons/second) emitted from xenograft tumors was quantified using Living Image Software (Caliper Life Sciences).

### Immunohistochemistry

Immunostaining was performed on 5 μm sections of xenograft tumor tissue preserved in either OCT compound or paraffin using the following antibodies: PECAM-1 (CD-31)(mAP-0032 Angio Proteomie, Boston, MA), anti-human α-smooth muscle actin (αSMA) antibody (A-2547, Sigma–Aldrich, St. Louis, MO), and type-IV collagen (LB-1403, Cosmo-Bio, Tokyo, Japan). Further details in Supplemental Materials.

Terminal deoxynucleotidyl transferase-mediated nick-end labeling (TUNEL) assay was performed using the ApopTag Red In Situ Apoptosis Detection kit (Millipore-Chemicon, Billerica, MA) on 5 μm sections of fresh frozen xenograft tumor tissue.

### Caspase 3/7 apoptosis luminescent assay

SH-SY5Y and SH-SY5Y.siP53 cells were plated in white walled 96 well plates (Corning Life Sciences, Lowell, MA) 24 h prior to the assay. Activation of apoptosis was measured with Caspase-Glo® 3/7 Assay (Promega Corporation, Madison, WI). Luminescence was detected with the Luminoskan Ascent Microplate Luminometer and analysis was performed with Ascent Software v2.6 (Thermo Fisher Scientific).

### Digital quantification of vasculature and apoptosis

Quantitative assessment of angiogenesis was performed by computer-assisted digital image analysis using Image Pro Software (Media Cybernetics, Bethesda, MD) as previously described [42]. Random high-power field digital images from immunostained xenograft tumor for vascular elements (CD-31, αSMA, type-IV collagen) and apoptosis (TUNEL) were analyzed and positive pixels quantified (see Supplemental Materials).

### Calculation of metastasis

*Incidence of metastasis*: For each mouse, 5 μm sections from three different levels of the liver were H+E stained and scored for metastasis using light microscopy (Leica DM5500B microscope, Leica DFC 360FX digital camera).

*Metastatic burden* was calculated by determining the area of the metastasis using Surveyor software (version 5.5.5.30, Objective Imaging, Cambridge, United Kingdom). An average area of metastasis (μm) was calculated for each mouse using data from three slides.

### Statistical analysis

Western blot analysis, qPCR, and ELISA were all performed in triplicate, and data was compared using Student's *t* test. Tumor weights were expressed as mean ± SEM. Xenograft tumor flux (photons/sec) ± SEM, measured by bioluminescent imaging, was compared using Student's t-test. Data from digital image analysis were expressed as mean ± SE and compared by Student's t-test. Incidence of metastasis was calculated by Fisher's exact test and metastatic burden was calculated by Kruskal–Wallis method.

## Results

### Nutlin-3a stabilizes p53 and suppresses HIF-1α expression

Human neuroblastoma cells from the cell line, SH-SY5Y, were treated under normoxic (21% O2) and hypoxic (1% O2) conditions with vehicle, Nutlin-3a, bevacizumab, and the combination of Nutlin-3a and bevacizumab. By Western blot analysis, Nutlin-3a stabilizes p53 expression levels, which induces a rebound increase in MDM2 expression (Supplemental Figure 1). This effect is seen in both Nutlin-3a treated and combination treated groups. Increase in p53 expression induces downstream p21 expression (Supplemental Figure 1). In addition to activating the p53 pathway, MDM2 inhibition leads to inhibition of HIF-1α expression (Fig. 1). Western blot analysis of treated SH-SY5Y cells demonstrates suppression of HIF-1α expression by Nutlin-3a when treated as a single agent or in combination with bevacizumab (Fig. 1A). Western blot densitometry verifies Nutlin-3a treatment significantly inhibits HIF-1α compared to control treatment (Fig. 1B).

### Nutlin-3a suppression of HIF-1α leads to p53-independent inhibition of VEGF

Quantitative real-time PCR was performed on treated SH-SY5Y cells and SH-SY5Y cells with p53 knockdown (SH-SY5Y.sip53, Fig. 2A) to determine VEGF mRNA expression (Fig. 2B). Under normoxic and hypoxic conditions, transcription of VEGF mRNA is inhibited by Nutlin-3a (single agent or in combination with bevacizumab). ELISA was performed on treated SH-SY5Y and SH-SY5Y.sip53 cells to determine expression of secreted VEGF. In SH-SY5Y cells, Nutlin-3a treatment leads to significant inhibition of VEGF expression (Fig. 2C). As expected, treatment with bevacizumab (as a single agent or in combination with Nutlin-3a) leads to nearly undetectable levels of secreted VEGF (Fig. 2C and 2D). To determine if Nutlin's effect on VEGF is dependent on p53, we performed ELISA for VEGF expression on

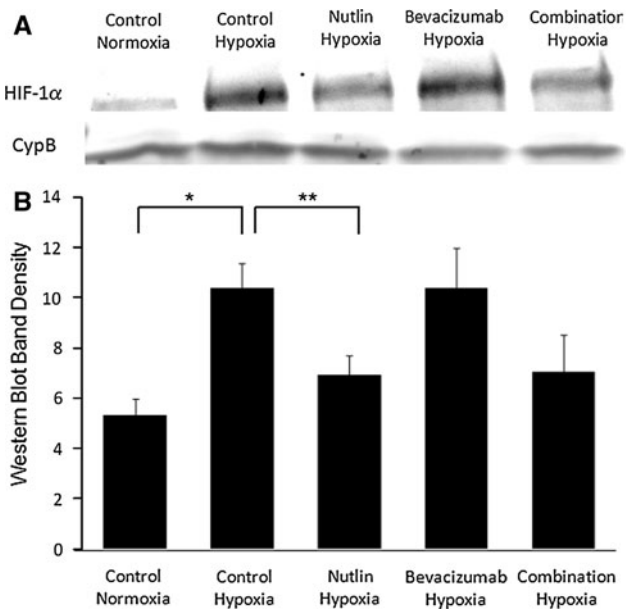


**Fig. 1** Nutlin-3a treatment suppresses HIF-1α expression. **a** Western blot analysis of treated SH-SY5Y cells for HIF-1α expression. Compared to control, Nutlin-3a treated cells (single agent or in combination with bevacizumab) leads to decreased expression of HIF-1α. **b** Western blot densitometry demonstrates significant increase in HIF-1α from normoxic to hypoxic conditions (* $P < 0.02$). Nutlin-3a treatment leads to significant decrease in HIF-1α expression (** $P < 0.05$)

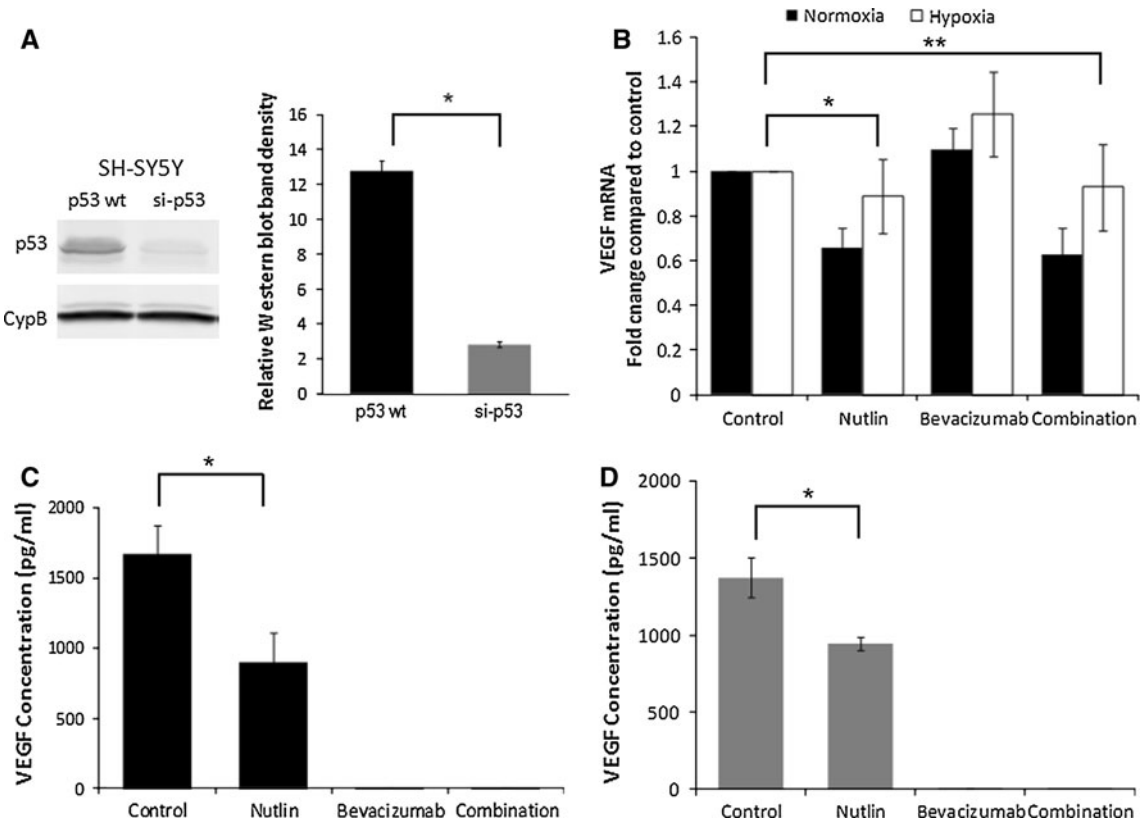


**Fig. 2** Nutlin-3a-mediated suppression of HIF-1α inhibits VEGF expression in a p53-independent fashion. SH-SY5Y neuroblastoma cells and SH-SY5Y cells with stable knockdown of p53 (SH-SY5Y.sip53) were treated under normoxic (21% O2) and hypoxic (1% O2) conditions with vehicle, Nutlin-3a, bevacizumab, and the combination of Nutlin-3a and bevacizumab. **a** Western blot analysis with band densitometry demonstrating 78% knockdown of p53 in SH-SY5Y.sip53 cell line compared to SH-SY5Y wild-type cell line (* $P < 0.004$). **b** Quantitative real-time PCR to detect mRNA transcription of VEGF in treated SH-SY5Y cells. Cells treated with Nutlin-3a (single agent or in combination with bevacizumab) demonstrated decreased VEGF mRNA transcription compared to control (* $P < 0.03$, ** $P < 0.04$). **c** By ELISA, Nutlin-3a significantly inhibits VEGF expression compared to control in treated SH-SY5Y cells (* $P < 0.02$). **d** In treated SH-SY5Y.sip53 cells, Nutlin-3a significantly inhibits secreted VEGF in the setting of p53 knockdown (* $P < 0.006$). As expected, all cells treated with bevacizumab (alone or in combination with Nutlin) have nearly undetectable levels of VEGF

treated SH-SY5Y.sip53 cells. Nutlin-3a treatment significantly inhibits VEGF expression in SH-SY5Y.sip53 cells, suggesting a p53-independent process (Fig. 2D).

## Comparison of treatment strategies on tumor growth in experimental neuroblastoma

To determine the combined effect of Nutlin-3a and bevacizumab on tumor growth and tumor angiogenesis, we employed a well-characterized xenograft model of neuroblastoma and monitored tumor growth by bioluminescent imaging [43]. After tumor implantation, mice were randomized and underwent treatment for 2 weeks. At the time of sacrifice, Nutlin-3a alone and bevacizumab alone tumors emit less flux than control tumors (Fig. 3A). Tumors treated with the combination of Nutlin-3a and bevacizumab demonstrate significantly less flux compared to control ($P < 0.05$). At necropsy, compared to control, Nutlin-3a and bevacizumab partially suppresses tumor growth by 57 and 44%, respectively ($P$ = not significant (NS) for both). However, combination treatment significantly suppresses tumor growth by 79% compared to control ($P < 0.02$) (Fig. 3B). Compared to bevacizumab alone, the addition of Nutlin-3a to bevacizumab significantly decreases tumor weight as well ($P$0.05). From this data, the combination of Nutlin-3a and bevacizumab more effectively inhibits xenograft tumor growth than either agent alone.

## Anti-angiogenic effect of Nutlin-3a and bevacizumab on neuroblastoma xenografts

The effect of the various treatment groups on angiogenesis was evaluated by immunostaining for CD-31 (PECAM), a marker of endothelial cells. CD-31 staining showed an abundance of endothelial cells and blood vessels in control tumors (Fig. 4A-i), a decrease in endothelial cell staining

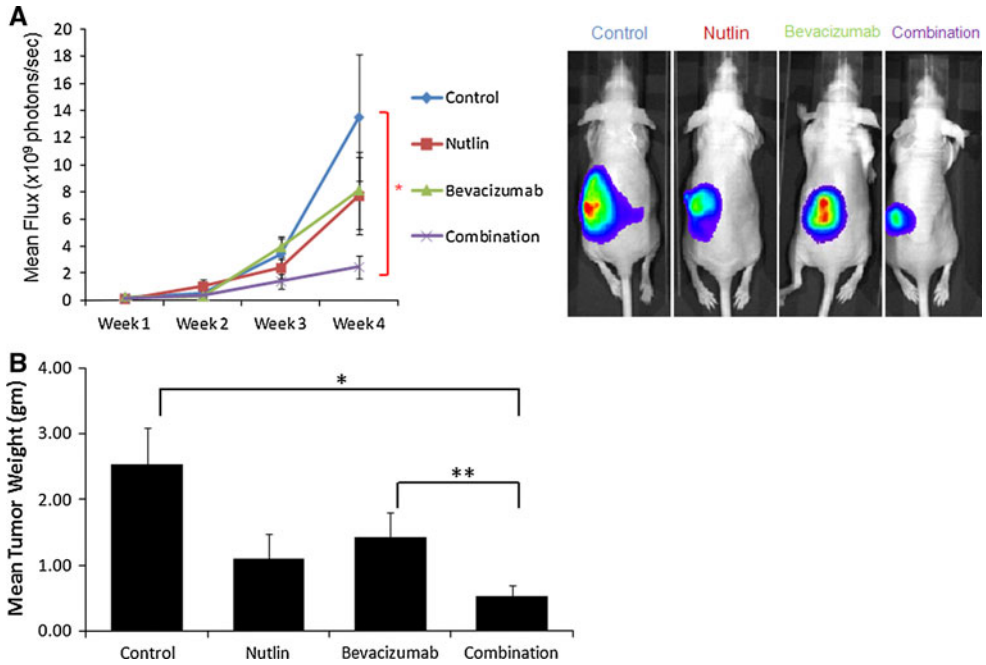


**Fig. 3** The effect of Nutlin-3a and bevacizumab on experimental neuroblastoma. Two weeks after tumor implantation, nude mice were randomly divided into four treatment cohorts and treated for 2 weeks: Control (vehicle) ($n = 10$), Nutlin-3a (200 mg/kg/dose, twice a day × 14 days) ($n = 10$), bevacizumab (5 mg/kg/dose, twice a week × 14 days) ($n = 10$), and combination of Nutlin-3a and bevacizumab ($n = 10$). **a** All mice underwent weekly monitoring of tumors by bioluminescent imaging. After 2 weeks of treatment, decreased flux (photons/second) was observed from Nutlin-3a and bevacizumab treated tumors (flux at 6 weeks (photons/seconds) ± SEM: control 1.35E+10 ± 4.67E+9, Nutlin-3a 7.70E+10 ± 2.90E+9, bevacizumab 8.11E+9 ± 2.84E+9; $P$ = NS for both). However, combination treated tumors demonstrated a significant decrease in flux when compared to vehicle control (combination 2.46E+9 ± 8.21E+8 photons/sec, * $P$ <0.05). Representative bioluminescent images from each treatment group are seen on the right. **b** After the treatment period, all mice were sacrificed, and tumors were resected and weighed. Xenograft tumor weight correlated with bioluminescent data (Fig. 3B). Nutlin-3a alone and bevacizumab alone partially suppresses xenograft tumor growth by 57 and 44%, respectively, compared to control (mean tumor weight in grams ± -SEM: control 2.54 ± 0.55 gm, Nutlin-3a 1.10 ± 0.37 gm, bevacizumab 1.42 ± 0.38 gm, $P$ = NS for both). Compared to control, combination treatment inhibited neuroblastoma xenograft tumor growth by 79% (combination 0.53 ± 0.16 gm, * $P < 0.02$). Combination treatment tumors were 62% smaller than the bevacizumab treated tumors (** $P < 0.05$). Bars represent mean tumor weight ± SEM

in Nutlin-3a-treated and bevacizumab-treated tumors (Fig. 4A-ii, 4A-iii), and a marked decrease in the combination-treated group (Fig. 4A-iv). Digital image analysis was used to quantify CD-31 staining. Compared to control tumors, there was significant suppression of microvessel density (MVD) by 25% in the Nutlin-3a group, 29% in the bevacizumab group, and 57% in the combination group (Fig. 4A-v). While Nutlin-3a and bevacizumab both demonstrate significant anti-angiogenic effect, combining the two agents significantly suppresses CD-31 staining compared to either treatment alone ($P < 0.0001$ for both). This data suggests that combination therapy cooperatively inhibits endothelial cell development in neuroblastoma.

## Effect of Nutlin-3a and bevacizumab on vascular assembly in neuroblastoma

In addition to CD-31 staining, we examined other critical aspects of angiogenesis, including the development of perivascular basement membrane (type-IV collagen staining) and the recruitment of vascular mural cells (VMC) (αSMA staining).

Compared to control, there was a slight increase in perivascular basement membrane with Nutlin-3a treatment ($P$ = NS), a decrease of 14% with bevacizumab treatment ($P$ = NS), and a significant decrease of 32% with combination therapy ($P < 0.04$) (Fig. 4B: i–v). As a single agent, Nutlin-3a and bevacizumab did not significantly alter perivascular basement membrane development compared to control tumors. However, combination treatment demonstrates significant suppression of perivascular basement membrane compared to control and to Nutlin alone ($P < 0.0006$).

Utilizing αSMA staining, there was a decrease in vascular mural cells of 16% with Nutlin-3a ($P$ = NS), 45% with bevacizumab alone ($P < 0.0001$), and 32% with combination treatment ($P < 0.004$) compared to control treatment (Fig. 4C: i-v).

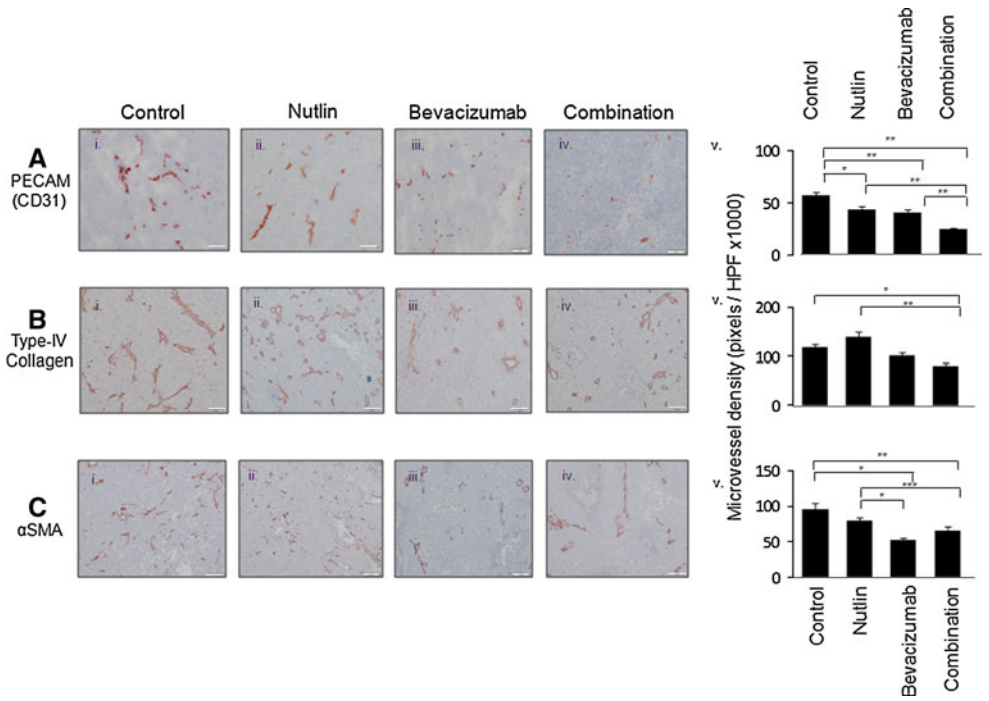


**Fig. 4** Immunohistochemical analysis of neuroblastoma xenografts after treatment with Nutlin-3a and bevacizumab. At the time of sacrifice, tumors were resected, preserved in paraformaldehyde and OCT compound, and then sectioned for immunohistochemical analysis. Angiogenesis was evaluated by immunostaining for the following vascular markers. **a** *i–iv* CD-31 (PECAM) staining for endothelial cells for each treatment group. Compared to control, combination treatment inhibits new blood vessel development more effectively than Nutlin-3a or bevacizumab alone. *v* Positive immunostaining was digitally quantified and measured as microvessel density (MVD) in pixels per HPF ± SEM for the following treatment groups: control 47,676 ± 2,711; Nutlin-3a 43,157 ± 2,889; bevacizumab 40,691 ± 2,325; combination 24,772 ± 1,404 (* $P < 0.0005$, ** $P < 0.0001$). Combination treatment show significantly less immunostaining compared to Nutlin-3a or bevacizumab alone. **b** *i–iv* Type-IV collagen staining for perivascular basement membrane for each treatment group. *v* Digital quantification of type-IV collagen in pixels/HPF ± SEM: control 117,722 ± 8,125; Nutlin-3a 140,715 ± 9,270; bevacizumab 100,701 ± 7,979; combination 79,513 ± 7,556. Bevacizumab combined with Nutlin-3a has a marked effect on perivascular basement membrane development as opposed to single agent treatment (* $P < 0.04$, ** $P < 0.0006$). **c** *i–iv* αSMA staining for differentiated vascular mural cells for each treatment group. *v* Digitally quantified staining for αSMA in pixels/HPF ± SEM: control 96,245 ± 8,280; Nutlin-3a 80,594 ± 3,745; bevacizumab 53,028 ± 2,805; combination 65,584 ± 5,819 (* $P < 0.0001$, ** $P < 0.004$, *** $P < 0.03$). Bevacizumab, alone or in combination with Nutlin-3a, has a potent inihibitory effect on vascular mural cell recruitment. All images taken at 10× objective, standard bar = 100 μm

Nutlin-3a alone does not appear to significantly alter the recruitment of VMCs compared to control ($P$ = NS), however, bevacizumab alone has a potent effect with significantly less VMC staining than control and Nutlin-3a alone ($P < 0.0001$ for both). Combination treatment also demonstrates significantly less VMC staining than control and Nutlin-3a alone treatments ($P < 0.004$, $P < 0.03$, respectively), which most likely represents a bevacizumab effect on VMC recruitment (Fig. 4C:v). From our data, bevacizumab has a significant effect on VMC recruitment, and this effect is not augmented by adding Nutlin-3a.

## Nutlin-3a and bevacizumab increase tumor apoptosis in neuroblastoma

By TUNEL immunostaining, Nutlin-3a treatment demonstrates a marked increase in apoptotic tumor cells by 240% ($P < 0.0001$), an increase of 94% by bevacizumab ($P < 0.0001$), and an increase of 175% by combination treatment ($P < 0.0001$) compared to control (Fig. 5A: i-v). Potent tumor apoptosis observed with Nutlin-3a treatment, through stabilization of p53, is strongly evident both in the Nutlin-3a group and in the combination group. While bevacizumab induces tumor cell apoptosis, presumably from hypoxia through its anti-angiogenic activity, it is significantly less than Nutlin-3a (Nutlin-3a versus bevacizumab, $P < 0.02$). Additionally, bevacizumab treatment does not appear to augment the tumor apoptotic activity of Nutlin-3a (Nutlin-3a versus combination, $P$ = NS).

In addition to Tdt, we assessed the apoptotic effect of the various treatments using an in vitro caspase assay (Fig. 5B). Compared to control, bevacizumab did not elicit an apoptotic effect, whereas Nutlin-3a, alone (>sixfold) or in combination with bevacizumab (>fivefold), demonstrated a significant increase in caspase activation

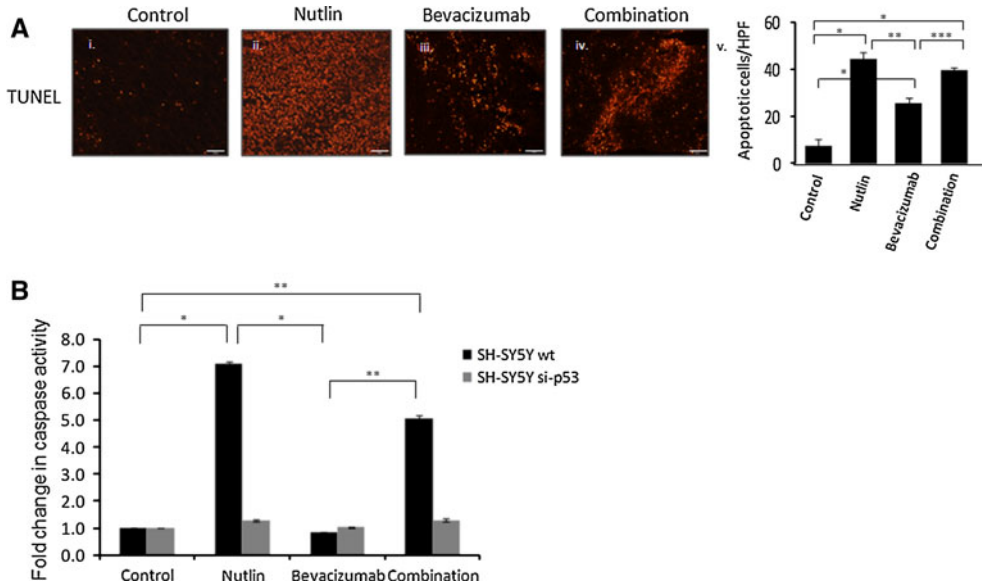


**Fig. 5** The effect of Nutlin-3a and bevacizumab on tumor apoptosis. **a** *i-iv* Apoptosis of xenograft tumors was evaluated by TUNEL immunostaining for each treatment group. v. Digital quantification of TUNEL-positive cells/HPF ± SEM: control 92 ± 4; Nutlin-3a 313 ± 53; bevacizumab 179 ± 15; combination 254 ± 19 (* $P <$ 0.0001, ** $P < 0.02$, *** $P < 0.003$). Apoptosis of orthotopic tumors is most pronounced in tumors treated with Nutlin-3a, either alone or in combination with bevacizumab. All images taken at 10× objective, standard bar = 100 μm. **b** Caspase assay of treated wild-type SH-SY5Y and SH-SY5Y.sip53 cells. Wild-type SH-SY5Y cells treated with Nutlin-3a, alone or in combination, demonstrate a marked increase in caspase activation compared to control or bevacizumab alone (* $P < 0.0003$, ** $P < 0.0008$). Knockdown of p53 in SH-SY5Y cells (SH-SY5Y.sip53) abolishes Nutlin-3a-mediated apoptosis, suggesting that it is p53 dependent

($P < 0.0003$ and $P < 0.0008$, respectively). Using the p53-knockdown cell line of neuroblastoma, there was no change in apoptosis in Nutlin-3a treated cells compared to control, thus suggesting that the mechanism of apoptosis is p53-dependent (Fig. 5B).

From this data, p53-mediated apoptosis by Nutlin-3a, alone or in combination with bevacizumab appears to be the dominant pathway in tumor apoptosis.

The effect of Nutlin-3a and bevacizumab on metastasis

At the time of sacrifice, livers were resected from all mice and embedded in paraffin. All liver sections were H&E stained for visual scoring of metastasis as described (see Supplemental Materials).

Control mice had a 67% incidence of metastasis while bevacizumab treated mice had metastases in 50%. Nutlin-3a treated mice and combination treated mice each had a significantly decreased incidence of metastasis of 20% each ($P < 0.05$) (Fig. 6A). Evaluation of total metastatic burden was calculated by digital image quantification of metastatic foci (Fig. 6B and 6C and see Supplemental Materials). Compared to control mice, Nutlin treated mice demonstrated 78% less metastatic burden ($P < 0.04$), bevacizumab 45% less metastatic burden ($P =$ NS), and combination treated mice greater than 95% less metastatic burden ($P < 0.03$) (Fig. 6B). While not significant, there was less metastatic burden in the combination treated mice than Nutlin alone.

We conclude that Nutlin-3a treatment alone and in combination significantly suppresses the incidence of metastasis in neuroblastoma as well as the metastatic burden.

## Discussion

Neuroblastoma is an aggressively invasive and metastatic extra-axial tumor which demonstrates pronounced angiogenesis and high vascularity. Yet anti-angiogenic treatments, specifically bevacizumab, have demonstrated limited responses in preclinical animal models and limited clinical trials [39, 43, 44]. Previous studies in other tumor types (e.g. lung [45], colorectal [36], renal [35], and breast cancer [37]) have shown that adjuvant chemotherapy can enhance the response to bevacizumab. The recent characterization of Nutlin as an MDM2 inhibitor which both promotes p53 stabilization and represses VEGF-mediated angiogenesis led us to assess the combination of Nutlin-3a with bevacizumab, using an orthotopic animal model of neuroblastoma.

We demonstrate that Nutlin-3a mediated tumor suppression results from its effects on two parallel tumorigenic pathways. First is the well-characterized stabilization of

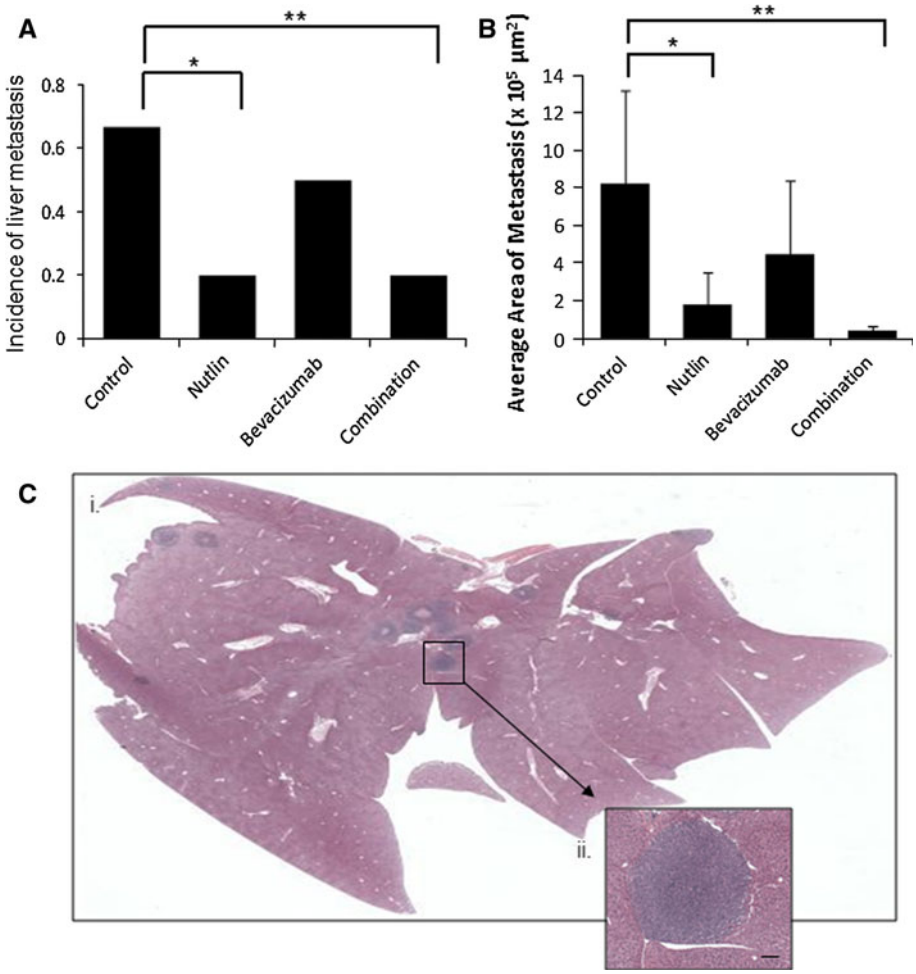


**Fig. 6** The effect of Nutlin-3a and bevacizumab on metastasis in an in vivo model of neuroblastoma. **a** Compared to control (67% incidence), the incidence of metastasis is significantly decreased by Nutlin-3a treatment (20%) and combination treatment (20%) (* $P < 0.05$). **b** Within liver sections analyzed, control mice had a calculated metastatic burden of 825,000 ± 492,000 μm$^2$ of tumor, and bevacizumab treated mice 450,000 ± 394,000 μm$^2$ of tumor ($P$ = NS). Nutlin-3a treatment and combination treatment demonstrate significantly less metastatic burden compared to control (Nutlin-3a 178,000 ± 174,000 μm$^2$; combination 39,000 ± 26,000 μm$^2$) (* $P < 0.04$, ** $P < 0.03$). **c** *i* A representative histologic image of a H&E stained liver. *i* Histologic sectioned image at 5× objective of an entire mouse liver using a novel software program to "stitch" multiple smaller images together. Areas of neuroblastoma metastases are distinct from hepatic parenchyma. One metastasis is outlined in the black box. *ii* Zoomed in view of the boxed metastasis at 10× objective. Standard bar = 100 μm

p53 and sensitization to apoptosis by MDM2 inhibition. We demonstrate marked in vivo p53-mediated tumor apoptosis in Nutlin-3a treated tumors by TUNEL immunostaining and in vitro by caspase activation assays.

The second MDM2-mediated pathway of tumor suppression is through inhibition of VEGF-mediated tumor angiogenesis. Our evaluation of tumor angiogenesis demonstrates a clear anti-angiogenic effect by Nutlin-3a, shown by CD-31 immunostaining. Our in vitro studies suggest that the anti-angiogenic properties of Nutlin-3a appear to be through suppression of HIF-1α and downstream VEGF transcription, and this effect is p53-independent. In vivo, we have also observed decreased VEGF transcription in Nutlin-treated xenografts (data not shown).

In addition to demonstrating anti-tumor and anti-angiogenic properties of Nutlin-3a, we sought to determine if MDM2 inhibition in combination with bevacizumab would have a cooperative effect on tumor suppression and angiogenesis by targeting the VEGF pathway at multiple sites. In our study, combination treatment demonstrates greater tumor suppression than either agent alone. Angiogenesis, as measured by CD-31 immunostaining, is suppressed most in the combination group than either single agent treatment group. This suggests that part of the cooperative effect of combination therapy is not only from anti-angiogenic mechanisms mediated by VEGF inhibition, but also by the anti-tumorigenic effect mediated by upregulation of the p53 apoptosis pathway.

In addition, we found that Nutlin-3a treatment, alone and in combination, had a potent effect on metastasis compared to control and bevacizumab treatment. While the incidence of metastasis was significantly less in Nutlin-treated mice (Nutlin-3a alone and combination), the metastatic burden was least in the combination group. This data suggests that while MDM2 and inhibition of p53 is critical to the initiation of metastasis, suppression of VEGF may limit the growth of metastatic foci.

Bevacizumab was the first FDA-approved anti-angiogenic drug for the treatment of cancer, and many other inhibitors of the VEGF pathway have since been developed. These include VEGF ligand inhibitors, such as VEGF Trap [46], and small molecule tyrosine kinase inhibitors which block VEGF receptors, such as sunitinib [47], sorafenib [48], and cediranib [49]. To date, these anti-angiogenic therapies have only been used in combination with chemotherapy, a genotoxic treatment. FDA approval was granted to bevacizumab after phase III trials showed increased efficacy of chemotherapy with the addition of bevacizumab in metastatic colorectal carcinoma and in non-small cell lung cancer [36, 45]. Newer agents, such as cediranib (small molecule tyrosine kinase inhibitor which blocks all three VEGF receptors), have also undergone phase I trials to look at the safety of combining novel anti-angiogenic therapies with a variety of chemotherapy regimens [50]. Additionally, anti-angiogenic drugs have been combined with ionizing radiation, another genotoxic therapy, in preclinical studies, which demonstrate a synergistic effect in non-small cell lung cancer and rhabdomyosarcoma animal models [51, 52]. Unique to this study is the sole use of two non-genotoxic therapies, which target two major tumorigenic pathways. Combining these two agents increased efficacy in suppressing tumor size, tumor angiogenesis, and distant metastasis. Importantly, by combining non-genotoxic therapies in patients, the risks and side effects of chemotherapy and radiation, namely secondary malignancies and marrow suppression with resulting neutropenia, may be averted.

In conclusion, we demonstrate for the first time that in addition to suppressing tumor growth through p53-mediated apoptosis, Nutlin-3a suppresses tumor angiogenesis through a distinct, p53-independent inhibition of VEGF in a murine model of neuroblastoma. Furthermore, our data validates the novel combination of Nutlin-3a with bevacizumab, which more effectively inhibited tumor growth and angiogenesis than either treatment alone. We also demonstrate for the first time that Nutlin-3a significantly suppresses tumor metastasis in a murine model of neuroblastoma, and that combination therapy may more effectively inhibit metastatic progression. These data suggest a novel therapeutic utility for MDM2 inhibitors, such as Nutlin-3a, as adjuncts to anti-angiogenic strategies for p53 wild-type and potentially p53 mutant tumors. Further optimization and clinical testing of this novel non-genotoxic combination therapy for highly vascular malignancies such as neuroblastoma are warranted.

**Acknowledgments** Funding support: Children's Neuroblastoma Cancer Foundation (EK); Hankamer Foundation, Baylor College of Medicine (EK); American Cancer Society Research Scholar grant RSG-07-209-01 (JS).

## References

1. Berthold F, Boos J, Burdach S, Erttmann R, Henze G, Hermann J, Klingebiel T, Kremens B, Schilling FH, Schrappe M, Simon T, Hero B (2005) Myeloablative megatherapy with autologous stem-cell rescue versus oral maintenance chemotherapy as consolidation treatment in patients with high-risk neuroblastoma: a randomised controlled trial. Lancet Oncol 6(9):649–658. doi:10.1016/S1470-2045(05)70291-6
2. Matthay KK, Villablanca JG, Seeger RC, Stram DO, Harris RE, Ramsay NK, Swift P, Shimada H, Black CT, Brodeur GM, Gerbing RB, Reynolds CP (1999) Treatment of high-risk neuroblastoma with intensive chemotherapy, radiotherapy, autologous bone marrow transplantation, and 13-cis-retinoic acid. Children's Cancer Group. N Engl J Med 341(16):1165–1173
3. Gurney JG, Tersak JM, Ness KK, Landier W, Matthay KK, Schmidt ML (2007) Hearing loss, quality of life, and academic problems in long-term neuroblastoma survivors: a report from the children's oncology group. Pediatrics 120(5):e1229–e1236. doi:10.1542/peds.2007-0178
4. Kushner BH, Kramer K, Modak S, Qin LX, Yataghena K, Jhanwar SC, Cheung NK (2009) Reduced risk of secondary leukemia with fewer cycles of dose-intensive induction chemotherapy in patients with neuroblastoma. Pediatr Blood Cancer 53(1):17–22. doi:10.1002/pbc.21931
5. Laverdiere C, Cheung NK, Kushner BH, Kramer K, Modak S, LaQuaglia MP, Wolden S, Ness KK, Gurney JG, Sklar CA (2005) Long-term complications in survivors of advanced stage neuroblastoma. Pediatr Blood Cancer 45(3):324–332. doi:10.1002/pbc.20331
6. Matthay KK, Reynolds CP, Seeger RC, Shimada H, Adkins ES, Haas-Kogan D, Gerbing RB, London WB, Villablanca JG (2009) Long-term results for children with high-risk neuroblastoma treated on a randomized trial of myeloablative therapy followed by 13-cis-retinoic acid: a children's oncology group study. J Clin Oncol 27(7):1007–1013. doi:10.1200/JCO.2007.13.8925
7. Haupt R, Garaventa A, Gambini C, Parodi S, Cangemi G, Casale F, Viscardi E, Bianchi M, Prete A, Jenkner A, Luksch R, Di Cataldo A, Favre C, D'Angelo P, Zanazzo GA, Arcamone G, Izzi GC, Gigliotti AR, Pastore G, De Bernardi B (1979) Improved survival of children with neuroblastoma between and 2005: a report of the Italian neuroblastoma registry. J Clin Oncol 28(14):2331–2338. doi:10.1200/JCO.2009.24.8351
8. Chen L, Malcolm AJ, Wood KM, Cole M, Variend S, Cullinane C, Pearson AD, Lunec J, Tweddle DA (2007) p53 is nuclear and functional in both undifferentiated and differentiated neuroblastoma. Cell Cycle 6(21):2685–2696
9. Vogan K, Bernstein M, Leclerc JM, Brisson L, Brossard J, Brodeur GM, Pelletier J, Gros P (1993) Absence of p53 gene mutations in primary neuroblastomas. Cancer Res 53(21):5269–5273

10. Freedman DA, Wu L, Levine AJ (1999) Functions of the MDM2 oncoprotein. Cell Mol Life Sci 55(1):96–107
11. Haupt Y, Maya R, Kazaz A, Oren M (1997) Mdm2 promotes the rapid degradation of p53. Nature 387(6630):296–299. doi:10.1038/387296a0
12. Kubbutat MH, Jones SN, Vousden KH (1997) Regulation of p53 stability by Mdm2. Nature 387(6630):299–303. doi:10.1038/387299a0
13. Momand J, Jung D, Wilczynski S, Niland J (1998) The MDM2 gene amplification database. Nucleic Acids Res 26(15):3453–3459
14. Schmidt MK, Tommiska J, Broeks A, van Leeuwen FE, Van't Veer LJ, Pharoah PD, Easton DF, Shah M, Humphreys M, Dork T, Reincke SA, Fagerholm R, Blomqvist C, Nevanlinna H (2009) Combined effects of single nucleotide polymorphisms TP53 R72P and MDM2 SNP309, and p53 expression on survival of breast cancer patients. Breast Cancer Res 11(6):R89. doi:10.1186/bcr2460
15. Perfumo C, Parodi S, Mazzocco K, Defferrari R, Inga A, Scarra GB, Ghiorzo P, Haupt R, Tonini GP, Fronza G (2009) MDM2 SNP309 genotype influences survival of metastatic but not of localized neuroblastoma. Pediatr Blood Cancer 53(4):576–583. doi:10.1002/pbc.22132
16. Willander K, Ungerback J, Karlsson K, Fredrikson M, Soderkvist P, Linderholm M (2010) MDM2 SNP309 promoter polymorphism, an independent prognostic factor in chronic lymphocytic leukemia. Eur J Haematol 85(3):251–256. doi:10.1111/j.1600-0609.2010.01470.x
17. Chien WP, Wong RH, Cheng YW, Chen CY, Lee H (2010) Associations of MDM2 SNP309, transcriptional activity, mRNA expression, and survival in stage I non-small-cell lung cancer patients with wild-type p53 tumors. Ann Surg Oncol 17(4):1194-1202. doi:10.1245/s10434-009-0853-2
18. Chen Z, Lin Y, Barbieri E, Burlingame S, Hicks J, Ludwig A, Shohet JM (2009) Mdm2 deficiency suppresses MYCN-Driven neuroblastoma tumorigenesis in vivo. Neoplasia 11(8):753–762
19. Van Maerken T, Ferdinande L, Taildeman J, Lambertz I, Yigit N, Vercruysse L, Rihani A, Michaelis M, Cinatl J Jr, Cuvelier CA, Marine JC, De Paepe A, Bracke M, Speleman F, Vandesompele J (2009) Antitumor activity of the selective MDM2 antagonist nutlin-3 against chemoresistant neuroblastoma with wild-type p53. J Natl Cancer Inst 101(22):1562–1574. doi:10.1093/jnci/djp355
20. Kim E, Shohet J (2009) Targeted molecular therapy for neuroblastoma: the ARF/MDM2/p53 axis. J Natl Cancer Inst 101(22):1527–1529. doi:10.1093/jnci/djp376
21. Vassilev LT, Vu BT, Graves B, Carvajal D, Podlaski F, Filipovic Z, Kong N, Kammlott U, Lukacs C, Klein C, Fotouhi N, Liu EA (2004) In vivo activation of the p53 pathway by small-molecule antagonists of MDM2. Science 303(5659):844–848. doi:10.1126/science.1092472
22. Chen F, Wang W, El-Deiry WS (2010) Current strategies to target p53 in cancer. Biochem Pharmacol 80(5):724–730. doi:10.1016/j.bcp.2010.04.031
23. Brown CJ, Lain S, Verma CS, Fersht AR, Lane DP (2009) Awakening guardian angels: drugging the p53 pathway. Nat Rev Cancer 9(12):862–873. doi:10.1038/nrc2763
24. Barbieri E, Mehta P, Chen Z, Zhang L, Slack A, Berg S, Shohet JM (2006) MDM2 inhibition sensitizes neuroblastoma to chemotherapy-induced apoptotic cell death. Mol Cancer Ther 5(9):2358–2365. doi:10.1158/1535-7163.MCT-06-0305
25. Chen D, Li M, Luo J, Gu W (2003) Direct interactions between HIF-1 alpha and Mdm2 modulate p53 function. J Biol Chem 278(16):13595–13598. doi:10.1074/jbc.C200694200
26. Nieminen AL, Qanungo S, Schneider EA, Jiang BH, Agani FH (2005) Mdm2 and HIF-1alpha interaction in tumor cells during hypoxia. J Cell Physiol 204(2):364–369. doi:10.1002/jcp.20406
27. Lee YM, Lim JH, Chun YS, Moon HE, Lee MK, Huang LE, Park JW (2009) Nutlin-3, an Hdm2 antagonist, inhibits tumor adaptation to hypoxia by stimulating the FIH-mediated inactivation of HIF-1alpha. Carcinogenesis 30(10):1768–1775. doi:10.1093/carcin/bgp196
28. Gordan JD, Simon MC (2007) Hypoxia-inducible factors: central regulators of the tumor phenotype. Curr Opin Genet Dev 17(1):71–77. doi:10.1016/j.gde.2006.12.006
29. Bardos JI, Chau NM, Ashcroft M (2004) Growth factor-mediated induction of HDM2 positively regulates hypoxia-inducible factor 1alpha expression. Mol Cell Biol 24(7):2905–2914
30. LaRusch GA, Jackson MW, Dunbar JD, Warren RS, Donner DB, Mayo LD (2007) Nutlin3 blocks vascular endothelial growth factor induction by preventing the interaction between hypoxia inducible factor 1alpha and Hdm2. Cancer Res 67(2):450–454. doi:10.1158/0008-5472.CAN-06-2710
31. Narasimhan M, Rose R, Ramakrishnan R, Zell JA, Rathinavelu A (2008) Identification of HDM2 as a regulator of VEGF expression in cancer cells. Life Sci 82(25–26):1231–1241. doi:10.1016/j.lfs.2008.04.004
32. Narasimhan M, Rose R, Karthikeyan M, Rathinavelu A (2007) Detection of HDM2 and VEGF co-expression in cancer cell lines: novel effect of HDM2 antisense treatment on VEGF expression. Life Sci 81(17–18):1362–1372. doi:10.1016/j.lfs.2007.08.029
33. Leung DW, Cachianes G, Kuang WJ, Goeddel DV, Ferrara N (1989) Vascular endothelial growth factor is a secreted angiogenic mitogen. Science 246(4935):1306–1309
34. Kim KJ, Li B, Winer J, Armanini M, Gillett N, Phillips HS, Ferrara N (1993) Inhibition of vascular endothelial growth factor-induced angiogenesis suppresses tumour growth in vivo. Nature 362(6423):841–844. doi:10.1038/362841a0
35. Yang JC, Haworth L, Sherry RM, Hwu P, Schwartzentruber DJ, Topalian SL, Steinberg SM, Chen HX, Rosenberg SA (2003) A randomized trial of bevacizumab, an anti-vascular endothelial growth factor antibody, for metastatic renal cancer. N Engl J Med 349(5):427–434. doi:10.1056/NEJMoa021491
36. Hurwitz H, Fehrenbacher L, Novotny W, Cartwright T, Hainsworth J, Heim W, Berlin J, Baron A, Griffing S, Holmgren E, Ferrara N, Fyfe G, Rogers B, Ross R, Kabbinavar F (2004) Bevacizumab plus irinotecan, fluorouracil, and leucovorin for metastatic colorectal cancer. N Engl J Med 350(23):2335–2342. doi:10.1056/NEJMoa032691
37. Miller KD, Chap LI, Holmes FA, Cobleigh MA, Marcom PK, Fehrenbacher L, Dickler M, Overmoyer BA, Reimann JD, Sing AP, Langmuir V, Rugo HS (2005) Randomized phase III trial of capecitabine compared with bevacizumab plus capecitabine in patients with previously treated metastatic breast cancer. J Clin Oncol 23(4):792–799. doi:10.1200/JCO.2005.05.098
38. Kreisl TN, Kim L, Moore K, Duic P, Royce C, Stroud I, Garren N, Mackey M, Butman JA, Camphausen K, Park J, Albert PS, Fine HA (2009) Phase II trial of single-agent bevacizumab followed by bevacizumab plus irinotecan at tumor progression in recurrent glioblastoma. J Clin Oncol 27(5):740–745. doi:10.1200/JCO.2008.16.3055
39. Glade Bender JL, Adamson PC, Reid JM, Xu L, Baruchel S, Shaked Y, Kerbel RS, Cooney-Qualter EM, Stempak D, Chen HX, Nelson MD, Krailo MD, Ingle AM, Blaney SM, Kandel JJ, Yamashiro DJ (2008) Phase I trial and pharmacokinetic study of bevacizumab in pediatric patients with refractory solid tumors: a Children's Oncology Group Study. J Clin Oncol 26(3):399–405. doi:10.1200/JCO.2007.11.9230
40. Secchiero P, Corallini F, Gonelli A, Dell'Eva R, Vitale M, Capitani S, Albini A, Zauli G (2007) Antiangiogenic activity of the MDM2 antagonist nutlin-3. Circ Res 100(1):61–69. doi:10.1161/01.RES.0000253975.76198.ff

41. Slack A, Chen Z, Tonelli R, Pule M, Hunt L, Pession A, Shohet JM (2005) The p53 regulatory gene MDM2 is a direct transcriptional target of MYCN in neuroblastoma. Proc Natl Acad Sci USA 102(3):731–736. doi:10.1073/pnas.0405495102
42. Wild R, Ramakrishnan S, Sedgewick J, Griffioen AW (2000) Quantitative assessment of angiogenesis and tumor vessel architecture by computer-assisted digital image analysis: effects of VEGF-toxin conjugate on tumor microvessel density. Microvasc Res 59(3):368–376. doi:10.1006/mvre.1999.2233
43. Kim ES, Serur A, Huang J, Manley CA, McCrudden KW, Frischer JS, Soffer SZ, Ring L, New T, Zabski S, Rudge JS, Holash J, Yancopoulos GD, Kandel JJ, Yamashiro DJ (2002) Potent VEGF blockade causes regression of coopted vessels in a model of neuroblastoma. Proc Natl Acad Sci USA 99(17):11399–11404. doi:10.1073/pnas.172398399
44. Benesch M, Windelberg M, Sauseng W, Witt V, Fleischhack G, Lackner H, Gadner H, Bode U, Urban C (2008) Compassionate use of bevacizumab (Avastin) in children and young adults with refractory or recurrent solid tumors. Ann Oncol 19(4):807–813. doi:10.1093/annonc/mdm510
45. Sandler A, Gray R, Perry MC, Brahmer J, Schiller JH, Dowlati A, Lilenbaum R, Johnson DH (2006) Paclitaxel-carboplatin alone or with bevacizumab for non-small-cell lung cancer. N Engl J Med 355(24):2542–2550. doi:10.1056/NEJMoa061884
46. Holash J, Davis S, Papadopoulos N, Croll SD, Ho L, Russell M, Boland P, Leidich R, Hylton D, Burova E, Ioffe E, Huang T, Radziejewski C, Bailey K, Fandl JP, Daly T, Wiegand SJ, Yancopoulos GD, Rudge JS (2002) VEGF-Trap: a VEGF blocker with potent antitumor effects. Proc Natl Acad Sci USA 99(17):11393–11398. doi:10.1073/pnas.172398299
47. Mendel DB, Laird AD, Xin X, Louie SG, Christensen JG, Li G, Schreck RE, Abrams TJ, Ngai TJ, Lee LB, Murray LJ, Carver J, Chan E, Moss KG, Haznedar JO, Sukbuntherng J, Blake RA, Sun L, Tang C, Miller T, Shirazian S, McMahon G, Cherrington JM (2003) In vivo antitumor activity of SU11248, a novel tyrosine kinase inhibitor targeting vascular endothelial growth factor and platelet-derived growth factor receptors: determination of a pharmacokinetic/pharmacodynamic relationship. Clin Cancer Res 9(1):327–337
48. Lyons JF, Wilhelm S, Hibner B, Bollag G (2001) Discovery of a novel Raf kinase inhibitor. Endocr Relat Cancer 8(3):219–225
49. Wedge SR, Kendrew J, Hennequin LF, Valentine PJ, Barry ST, Brave SR, Smith NR, James NH, Dukes M, Curwen JO, Chester R, Jackson JA, Boffey SJ, Kilburn LL, Barnett S, Richmond GH, Wadsworth PF, Walker M, Bigley AL, Taylor ST, Cooper L, Beck S, Jurgensmeier JM, Ogilvie DJ (2005) AZD2171: a highly potent, orally bioavailable, vascular endothelial growth factor receptor-2 tyrosine kinase inhibitor for the treatment of cancer. Cancer Res 65(10):4389–4400. doi:10.1158/0008-5472.CAN-04-4409
50. Lorusso P, Shields AF, Gadgeel S, Vaishampayan U, Guthrie T, Puchalski T, Xu J, Liu Q (2010) Cediranib in combination with various anticancer regimens: results of a phase I multi-cohort study. Invest New Drugs. doi:10.1007/s10637-010-9484-5
51. Loriot Y, Mordant P, Dorvault N, De la Motte Rouge T, Bourhis J, Soria JC, Deutsch E (2010) BMS-690514, a VEGFR and EGFR tyrosine kinase inhibitor, shows anti-tumoural activity on non-small-cell lung cancer xenografts and induces sequence-dependent synergistic effect with radiation. Br J Cancer 103(3):347–353. doi:10.1038/sj.bjc.6605748
52. Myers AL, Williams RF, Ng CY, Hartwich JE, Davidoff AM (2010) Bevacizumab-induced tumor vessel remodeling in rhabdomyosarcoma xenografts increases the effectiveness of adjuvant ionizing radiation. J Pediatr Surg 45(6):1080–1085. doi:10.1016/jjpedsurg.2010.02.068